Engineering and Applied Science Letters

PSR Press

Article

Robust DC bus voltage regulation in a PEM fuel cell system using a PI-controlled two-phase interleaved boost converter

Ameze Big-Alabo[1,2,*]

[1] E. ON Energy Research Center, RWTH Aachen University, Germany
[2] Department of Electrical/Electronic Engineering, Faculty of Engineering, University of Port Harcourt, PMB 5323, Port Harcourt, Rivers State, Nigeria
* Correspondence: ameze.big-alabo@eonerc.rwth-aachen.de

Received: 24 February 2026; Accepted: 19 June 2026; Published: 22 June 2026.

Abstract: The present research studies the robust control of DC bus voltage in a proton-exchange membrane fuel cell (PEMFC)-fed power system using two-phase interleaved boost converter. The two-phase interleaved boost converter uses as a source two series-connected 6 kW PEMFC stacks that produce low-voltage DC source, which is converted to the stable 400V DC bus. The voltage control of the boost converter is realized by a simple proportional-integral voltage controller, which provides a duty-cycle signal for phase-shifted pulse-width modulation of the converter. The performance of the system is analyzed during variations of load demand, atmospheric pressure, and source/load disturbance. It is shown that the interleaved boost converter ensures the constant voltage level of the bus at 400V under step-changes of the load power and under decrease of the pressure from 1.0 bar to 0.3 bar. The decrease of the fuel cell voltage with increase of the load current and with decreasing of reactant pressure is compensated by adjusting the duty cycle of the converter and preventing the voltage collapse of the DC bus.

Keywords: PEM fuel cell, interleaved boost converter, PI voltage control, DC bus regulation, load disturbance, atmospheric pressure disturbance

1. Introduction

Fuel cells with proton-exchange membrane, called PEMFCs, are promising sources of energy for electricity conversion since they work at a relatively low temperature, have quick start-up characteristics, and generate DC energy with low local emissions. This makes PEMFCs appropriate for use in transportation, distributed generation, and DC microgrids. Nevertheless, the voltage output of such sources is normally low and dependent on the current of the load, supply of reactants, their pressure, temperature, and hydration level of the membrane [1–3]. Consequently, a power conditioning stage must be implemented between the fuel cell and the DC bus so that the voltage of the load would be stable while the electrochemical source is protected from the excessive current ripples and fast changes of current [1–3].

Interleaved boost converters are among the types of DC-DC converters that are appropriate for fuel cell systems since they split the input current into several phases and shift gate pulses of the converter phases. It leads to the decreased net input current ripples, reduced stress of semiconductor elements and inductors, enhanced thermal management, and higher power capability than a single phase converter with the same ratings [4–8]. In the case of a PEMFC source, lower ripples are particularly important since fast ripples of the source current can increase electrochemical stress of the source and deteriorate its performance and lifetime.

Control of an interleaved boost converter fed by a PEMFC is difficult since the source and the load may vary simultaneously. Load variations increase the converter current demands and lead to voltage drops due to the internal resistance and polarization losses of the fuel cell stack. Changes in environmental parameters, especially decrease in the operating pressure, affect the partial pressures of reactants and lead to the decreased reversible voltage of the cell according to the Nernst relationship. Previously, conventional PI or PID control, robust voltage control, sliding mode control, fractional order PID control, adaptive disturbance rejection, and optimization based regulators were analyzed for the PEMFC converter systems [9–15]. It was shown that

disturbance rejection is powerful, but many advanced regulators imply complicated models and increased tuning and computation efforts.

The question arises whether a simple PI voltage regulator is able to ensure the maintenance of high DC bus voltage in the case when a PEMFC source experiences both load changes and pressure reduction. It is important since there are some practical systems, such as electric vehicles and standalone DC microgrids, which have varying load demands and operate in variable ambient conditions. The literature also shows that fuel cell voltage depends on pressure, temperature, and gas composition [16–18]. That is why the effect of pressure reduction must be taken into account together with the load transients and not considered separately as a source parameter.

The aim of this research is to analyze a model of a 12 kW PEMFC DC system with a PI-controlled two-phase interleaved boost converter in three cases: load transients at constant pressure, pressure transients at constant load, and simultaneous load and pressure transients. It is necessary to find out whether the closed loop converter ensures the maintenance of DC bus voltage at 400 V when the PEMFC voltage varies due to the electrochemical and load factors.

2. Modelling of PEM fuel cell and two-phase interleaved boost converter

2.1. Modelling of PEM fuel cell

A control-oriented PEMFC model is needed to describe how the source voltage changes with current demand and environmental conditions. The terminal voltage of a PEMFC stack can be written as the reversible thermodynamic voltage minus activation, ohmic, and concentration losses. For a stack containing N_{cell} cells connected in series, the stack voltage is expressed as

$$V_{\text{stack}} = N_{\text{cell}} \left(E_{\text{Nernst}} - V_{\text{act}} - V_{\Omega} - V_{\text{conc}} \right), \tag{1}$$

where E_{Nernst} is the reversible cell voltage, V_{act} is the activation overpotential associated with electrode reaction kinetics, V_{Ω} is the ohmic voltage drop caused by ionic and electronic resistances, and V_{conc} is the concentration overpotential associated with mass-transport limitations [2,3].

For system-level converter design, the same voltage behaviour can be represented in compact form as

$$V_{\text{FC}} = E - IR_{\text{int}} - V_{\text{loss}}, \tag{2}$$

where V_{FC} is the fuel-cell terminal voltage, E is the open-circuit electrochemical voltage, I is the stack current, R_{int} is the equivalent internal resistance, and V_{loss} collects the activation and concentration losses. Eq. (2) explains the main voltage trends observed in the dynamic results: an increase in load current increases IR_{int}, while a reduction in reactant pressure lowers E and increases mass-transport limitations.

The pressure dependence of the reversible voltage is described by the Nernst equation,

$$E = E^0 + \frac{RT}{2F} \ln \left(\frac{P_{H_2} \sqrt{P_{O_2}}}{P_{H_2O}} \right), \tag{3}$$

where E^0 is the standard reversible potential, R is the universal gas constant, T is the absolute temperature, F is Faraday's constant, and P_{H_2}, P_{O_2}, and P_{H_2O} are the partial pressures of hydrogen, oxygen, and water vapour, respectively. A pressure reduction lowers the available oxygen partial pressure and therefore reduces the reversible voltage. This mechanism is consistent with PEMFC pressure-sensitivity studies that relate pressure, temperature, and water content to electrochemical performance [16–18].

2.2. Two-phase interleaved boost converter

A two-phase interleaved boost converter is used to connect the PEMFC source to the regulated DC bus. Each phase contains an inductor, a controlled switch, and a diode path to the output capacitor and load. The two switches operate with the same duty ratio and a phase displacement of 180°, so the input current is shared between the two inductors and the ripple components partially cancel at the fuel-cell terminals [4,19,20].

Under continuous conduction mode and ideal steady-state assumptions, the boost-converter voltage conversion relation is

$$\frac{V_o}{V_{\text{in}}} = \frac{1}{1-D}, \tag{4}$$

where V_o is the output DC bus voltage, V_{in} is the PEMFC input voltage to the converter, and D is the duty ratio. The nominal duty ratio corresponding to a 90 V input and a 400 V bus is approximately $D = 0.775$.

The steady-state power balance can be written as

$$P_o = V_o I_o = \eta V_{\text{in}} I_{\text{in}}, \tag{5}$$

where P_o is the output power, I_o is the output current, I_{in} is the source current, and η is the converter efficiency. For an N-phase interleaved converter, the average current in each phase is

$$I_{L,k,\text{avg}} = \frac{I_{\text{in}}}{N}, \qquad k = 1, 2, \ldots, N. \tag{6}$$

For the two-phase case, Eq. (6) indicates that each inductor carries approximately half of the input current under balanced operation. This current sharing reduces conduction stress and supports stable voltage regulation under transient loading.

3. Methodology

3.1. System configuration

The investigated PEMFC power system is shown in Figure 1. The source is composed of two PEMFC stacks connected in series. Each stack is rated at 6 kW, giving a total nominal power of 12 kW. The series connection raises the input voltage available to the boost converter, while the two-phase interleaved converter raises and regulates the output at a 400 V DC bus. A single outer voltage loop measures the DC bus voltage, compares it with the reference voltage, and updates the converter duty command through a PI controller.

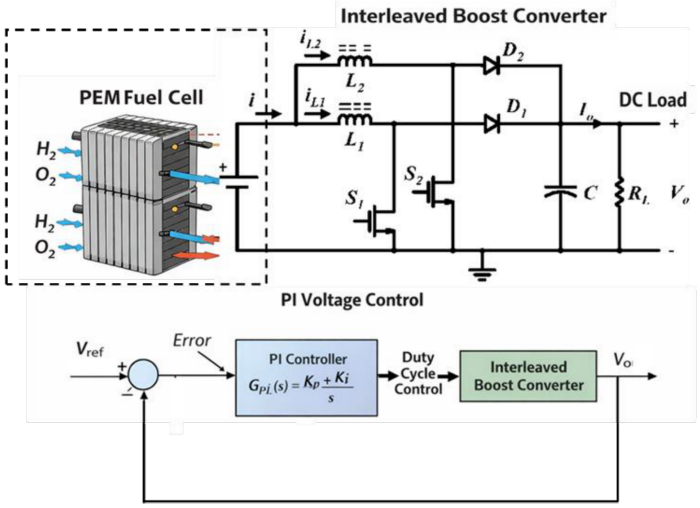

Figure 1. PEMFC-fed two-phase interleaved boost converter with PI voltage regulation

The PEMFC and DC bus specifications used for the converter design are listed in Table 1. These values define the nominal electrical operating point for the control and converter sizing calculations.

Table 1. Nominal PEMFC system specifications

Parameter	Symbol	Value	Unit
Number of PEMFC stacks	–	2	–
Rated power per stack	P_{stack}	6	kW
Total rated power	P_{in}	12	kW
Nominal stack voltage	V_{stack}	45	V
Total nominal input voltage	V_{in}	90	V
Input current at 12 kW	I_{in}	133	A
DC bus reference voltage	V_o	400	V
Output current at 12 kW	I_o	30	A

The main converter parameters are summarized in Table 2. The design uses two interleaved phases, a 180° phase shift, and a switching frequency of 5 kHz. The output-voltage ripple entry is reported as 1% because the selected 4 V ripple allowance corresponds to 1% of the 400 V bus.

Table 2. Two-phase interleaved boost converter design parameters

Parameter	Symbol	Value	Unit
Number of phases	N	2	–
Phase shift	ϕ	180	degree
Nominal duty ratio	D	0.775	–
Average inductor current per phase	$I_{L,\text{avg}}$	66.7	A
Current ripple ratio	r_L	20	%
Inductor ripple current per phase	ΔI_L	13.3	A
Switching frequency	f_s	5	kHz
Inductance per phase	L	1	mH
Voltage ripple ratio	r_C	1	%
Allowed voltage ripple	ΔV_o	4	V
Output capacitance	C	680	μF

3.2. PI voltage-control structure

The control objective is to maintain the DC bus at $V_{\text{ref}} = 400$ V despite changes in load power and source voltage. The measured output voltage V_o is subtracted from the reference voltage to form the error signal. This error is processed by a PI compensator,

$$G_{\text{PI}}(s) = K_p + \frac{K_i}{s}, \tag{7}$$

where K_p improves transient response and K_i removes steady-state error. The controller output is converted to a duty-cycle command and applied to the two PWM channels with a 180° phase displacement. The interleaving reduces the effective input ripple, while the PI loop corrects bus-voltage deviations caused by load steps or fuel-cell voltage changes. This combination allows the converter to regulate the load-side bus without requiring a high-order nonlinear controller [1,9,10].

4. Results and discussion

Dynamic performance is investigated in three operation cases. In the first case, DC load-power step changes occur with constant 1.0 bar atmospheric pressure. In the second case, pressure reduction from 1.0 bar to 0.3 bar is applied under the condition of constant load. In the last case, the pressure reduction is combined with load-power steps. The fuel-cell voltage will be used to evaluate the source-side stresses. The DC bus voltage is applied to analyze the load-side dynamic performance.

4.1. Load power variations at constant atmospheric pressure

The first experiment evaluates the ability of the system to regulate the bus voltage at the reference level when there are step changes in load power at constant pressure. Figure 2 displays the load-power step inputs and the corresponding fuel-cell voltage outputs.

4.1.1. Fuel-cell voltage response to load-power variation

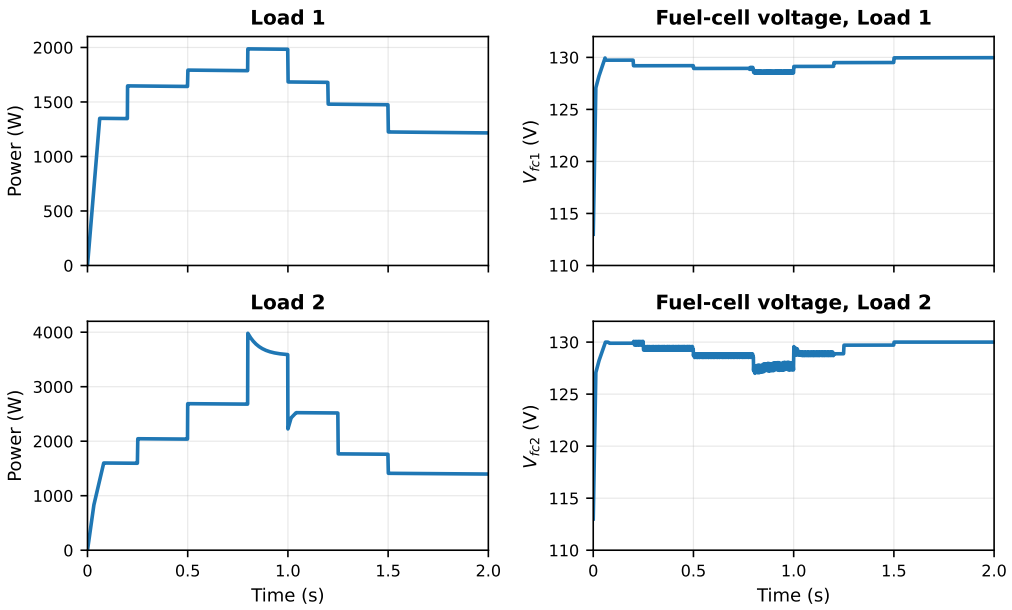

Figure 2. Load-power profiles and corresponding PEMFC voltage responses at constant atmospheric pressure

The fuel-cell voltage decreases with an increase of load because a higher load intensity causes additional voltage drops related to activation and ohmic losses in Eq. (2). With the lower-power load 1 input, the fuel-cell voltage remains almost stable after the start-up transient period because it means that the converter requests current within the capability of fuel-cell source without any source side stresses. With the higher-power load 2 input, the fuel-cell voltage demonstrates more distinct dips and a greater high-frequency component during the high-demand interval because there are more activation and ohmic losses in the fuel cell stack. The important point is that the fuel-cell voltage doesn't collapse, it means that the closed-loop controlled converter doesn't request unattainable currents under load steps.

4.1.2. DC bus voltage response to load variation

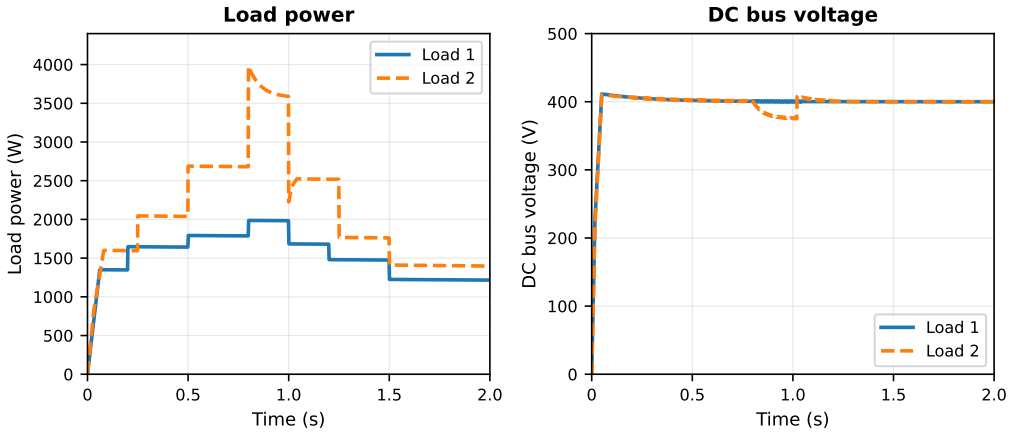

Figure 3. Load-power variation and regulated DC bus voltage for the two load profiles

The bus-voltage response in Figure 3 demonstrates an efficient performance of the load-side regulation. After the start-up transient, the DC bus voltage maintains a close level to the 400 V reference even with load-power step changes. With the higher-power load 2 input, there is a little deviation in the bus voltage, but it is a temporary one because the converter increases the duty ratio to provide load demand. Therefore,

the bus voltage returns to the regulated value without any oscillations, which proves that the PI controller and the interleaved power stage give sufficient dynamic damping properties to maintain the regulation.

4.2. Pressure variation at constant DC load

The second experiment isolates the effect of source-side pressure reduction. The pressure remains at 1.0 bar in the first atmospheric input case and is reduced from 1.0 bar to 0.3 bar at $t = 1$ s in the second atmospheric input case. This experiment is interesting because the pressure affects directly the oxygen partial pressure and therefore the reversible voltage in Eq. (3).

4.2.1. DC bus voltage response to atmospheric-pressure variation

Figure 4 illustrates that the DC bus voltage remains tightly regulated near 400 V level with the pressure reduction. Under the low-pressure case, the bus voltage experiences only slight transient effects because of the PI controller, which increases the converter duty ratio to compensate the decrease in the source voltage. This fact is important because the bus voltage is the voltage which is supplied to the load. This result means that the load is effectively decoupled from the electrochemical pressure disturbance over the simulated interval.

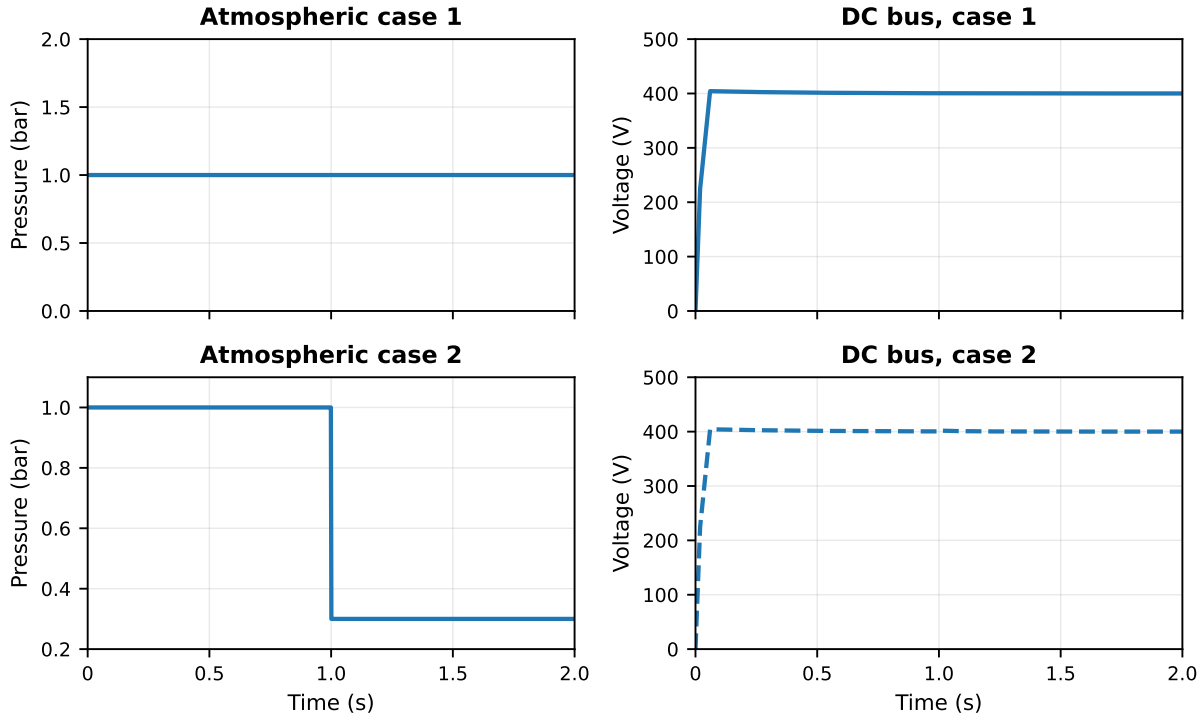

Figure 4. Atmospheric-pressure inputs and DC bus voltage responses under constant load

4.2.2. Fuel-cell voltage response to atmospheric-pressure variation

The source-side response in Figure 5 illustrates the physical impact of the pressure reduction. At constant pressure equal to 1.0 bar, the fuel-cell voltage remains steady after the start-up transient. When pressure reduces to 0.3 bar, the fuel-cell voltage settles at a lower voltage level, it is explained by Eq. (3). This equation states that the fuel-cell voltage reduces with the decrease in the oxygen partial pressure. The simultaneous analysis of Figures 4 and 5 shows that the converter keeps the bus voltage regulation even under the pressure disturbance.

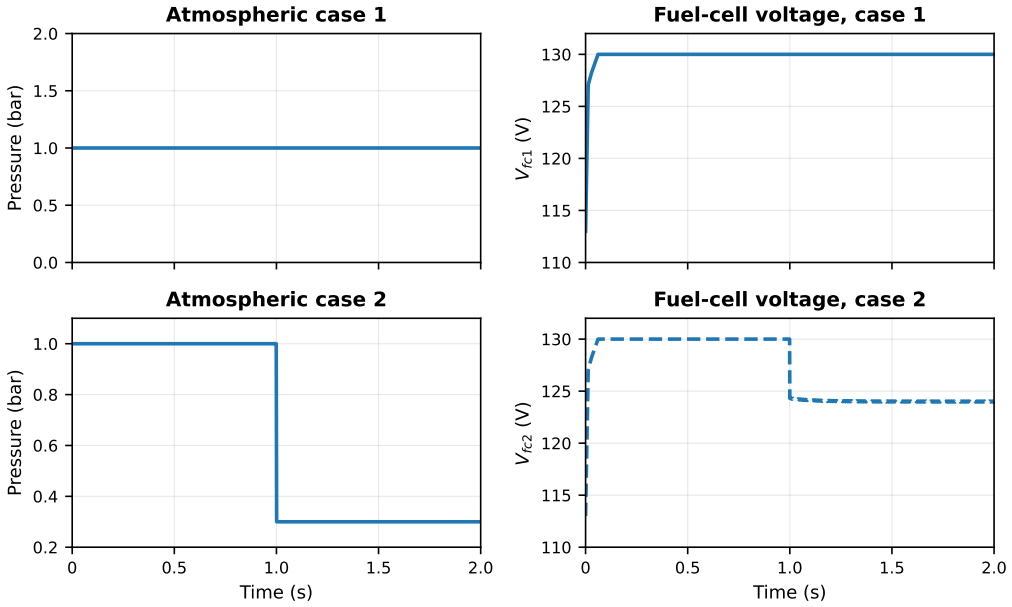

Figure 5. Atmospheric-pressure inputs and corresponding fuel-cell voltage responses

4.3. Combined atmospheric-pressure and DC-load variations

The third experiment applies the most extreme operating conditions considered in this paper. Pressure reduction from 1.0 bar to 0.3 bar at $t = 1$ s and the load-power variation are applied simultaneously. This experiment evaluates the ability of the system to regulate the bus voltage when the source capability and the load demand vary together.

4.3.1. Fuel-cell voltage response to combined disturbances

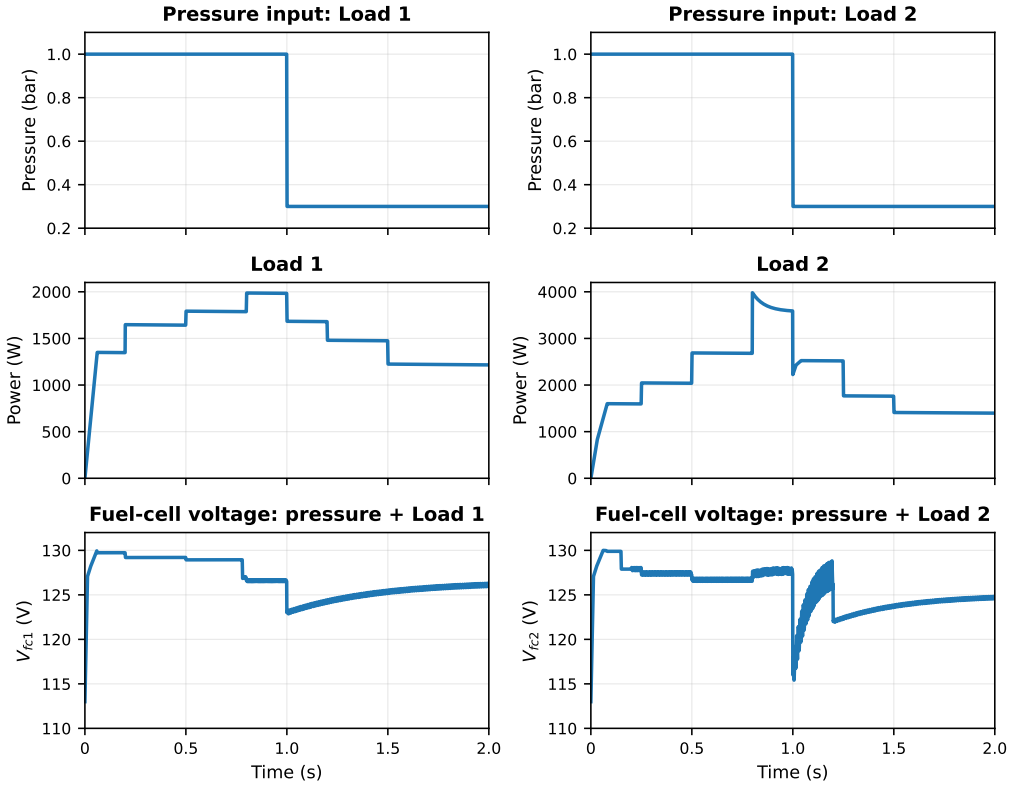

Figure 6. Fuel-cell voltage response under simultaneous pressure reduction and load variation

The combined response in Figure 6 shows that the fuel-cell voltage depends on the load current and reactant pressure. Before the pressure reduction step, load increases cause the moderate fuel-cell voltage reduction caused by the current-dependent voltage drop in Eq. (2). After the pressure drops, the fuel-cell voltage reduces more sharply because there are the open-circuit voltage reduction and the persistent current demand. Load 1 causes higher output voltage level than load 2 after the pressure reduction because of a smaller current stress on the fuel cell stack.

4.3.2. DC bus voltage response to combined disturbances

The DC bus response in Figure 7 is the strongest evidence of closed-loop robustness. Even when the fuel-cell voltage drops due to reduced pressure and the load profile changes at the same time, the bus voltage remains close to the 400 V reference. The larger Load 2 case produces a slightly more pronounced bus-voltage deviation than Load 1 because the converter must handle both a lower source voltage and a higher current demand. The deviation is corrected without growing oscillations, which indicates that the PI controller has sufficient damping for the tested disturbance magnitude. Therefore, the interleaved topology and voltage loop together provide the required energy-transfer adjustment between the PEMFC source and the regulated DC load.

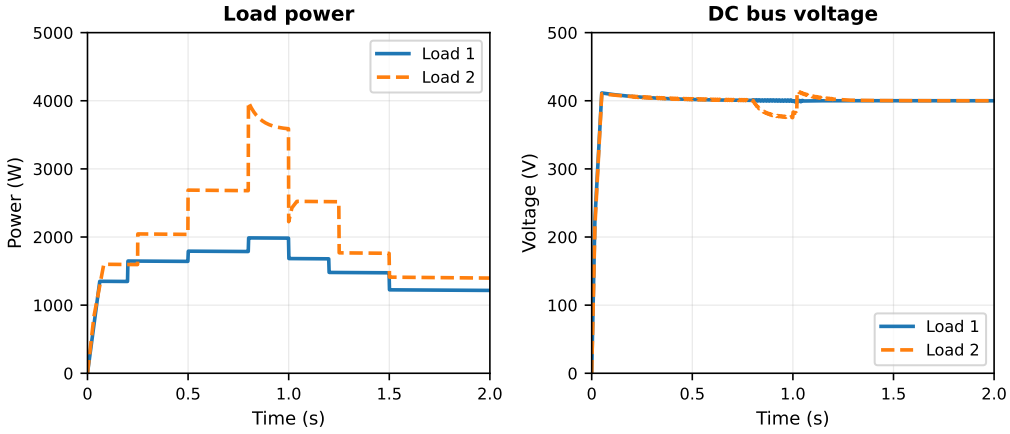

Figure 7. Load power and DC bus voltage under simultaneous pressure reduction and load variation

It is apparent from the presented plots that the results are indicative of a clear distinction between the source-side and load-side effects on the system behavior. The voltage of the PEMFC is permitted to reach a new operational level upon changing pressure, while the output voltage of the converter remains fixed due to the controlled operation of the DC bus. In practical terms, this is crucial since it is impossible to assume that the fuel cell acts as an ideal voltage source; thus, a properly stable converter must account for any variations in its voltage level and provide regulated bus voltage. It is clear from the provided responses that the chosen PI-controlled interleaved boost converter is capable of doing that for the particular test cases.

5. Conclusion

The problem addressed in this study was related to the ability of a PI-controlled two-phase interleaved boost converter to keep a 400 V DC bus regulated for the PEMFC power system during load variation, atmospheric-pressure reduction, and both source-side and load-side disturbances. The results have shown that the chosen solution allows solving this task positively. Upon load variation at the fixed value of pressure, the fuel-cell voltage decreased as expected under the load current; however, the DC bus was successfully regulated after the transients. Under the pressure reduction from 1.0 bar to 0.3 bar, the voltage of the PEMFC decreased due to the lower pressure of the reactants; however, the bus voltage was kept close to the 400 V set point. Simultaneous load and pressure variation led to the greatest decrease in the fuel-cell voltage, especially in the case of the high-power load profile; however, the converter managed to avoid bus-voltage collapse and restore the regulated level.

The main result of the work lies in the demonstration of the possibility of practical disturbance rejection in a PEMFC-powered DC system based on a two-phase interleaved boost converter with a well-designed PI voltage loop without the need for a complex controller. In this way, the interleaving topology provides the reduction of the current ripples and distribution of the currents, while the PI controller compensates for the voltage degradation and power variations by controlling the duty cycle of the switches.

The limitations of the study are associated with the simulation approach and the examination of the operation of the model under specific operating conditions. The extended work under the conditions of low pressure may lead to increased reactant demand and thermal and mechanical stress, and the further PEMFC degradation, which requires experimental verification of the PEMFC models and hardware testing.

Acknowledgments: The author acknowledges Dr. Akuro Big-Alabo for encouragement, constructive comments, and proofreading support. The author also acknowledges the Alexander von Humboldt Foundation for supporting the research fellowship of which this work forms a part.

Data Availability: All data used to support the findings of this study are presented in the manuscript.

Conflicts of Interest: The author declares no conflict of interest.

References

[1] Wang, C., Nehrir, M. H., & Gao, H. (2006). Control of PEM fuel cell distributed generation systems. *IEEE Transactions on Energy Conversion, 21*(2), 586-595.

[2] Asl, S. S., Rowshanzamir, S., & Eikani, M. H. (2010). Modelling and simulation of the steady-state and dynamic behaviour of a PEM fuel cell. *Energy, 35*(4), 1633-1646.

[3] Jia, J., Li, Q., Wang, Y., Cham, Y. T., & Han, M. (2009). Modeling and dynamic characteristic simulation of a proton exchange membrane fuel cell. *IEEE Transactions on Energy Conversion, 24*(1), 283-291.

[4] Thounthong, P., Sethakul, P., Rael, S., & Davat, B. (2008, April). Design and implementation of 2-phase interleaved boost converter for fuel cell power source. In *4th IET International Conference on Power Electronics, Machines and Drives* (PEMD 2008) (pp. 91-95). Stevenage UK: IET.

[5] Farhani, S., N'Diaye, A., Djerdir, A., & Bacha, F. (2020). Design and practical study of three phase interleaved boost converter for fuel cell electric vehicle. *Journal of Power Sources, 479*, 228815.

[6] Hegazy, O., Van Mierlo, J., & Lataire, P. (2011). Analysis, control and comparison of DC/DC boost converter topologies for fuel cell hybrid electric vehicle applications. In *Proceedings of the 14th European Conference on Power Electronics and Applications* (pp. 1–10).

[7] Seyezhai, R., & Mathur, B. L. (2012). Design and implementation of interleaved boost converter for fuel cell systems. *International Journal of Hydrogen Energy, 37*(4), 3897-3903.

[8] Benyahia, N., Denoun, H., Badji, A., Zaouia, M., Rekioua, T., Benamrouche, N., & Rekioua, D. (2014). MPPT controller for an interleaved boost dc–dc converter used in fuel cell electric vehicles. *International Journal of Hydrogen Energy, 39*(27), 15196-15205.

[9] Miranda, M., Chetan, M., Dsouza, N. S., & Chetan, N. P. (2021, May). Robust Voltage Control of Two-Phase Interleaved Boost Converter for Fuel Cell Systems. In *2021 Emerging Trends in Industry 4.0* (ETI 4.0) (pp. 1-6). IEEE.

[10] Huangfu, Y., Zhuo, S., Chen, F., Pang, S., Zhao, D., & Gao, F. (2017). Robust voltage control of floating interleaved boost converter for fuel cell systems. *IEEE Transactions on Industry Applications, 54*(1), 665-674.

[11] Zhuo, S., Xu, L., Huangfu, Y., Gaillard, A., Paire, D., & Gao, F. (2021). Robust adaptive control of interleaved boost converter for fuel cell application. *IEEE Transactions on Industry Applications, 57*(6), 6603-6610.

[12] Yasin, A., Yasin, A. R., Saqib, M. B., Zia, S., Riaz, M., Nazir, R., ... & Bajwa, S. (2022). Fuel cell voltage regulation using dynamic integral sliding mode control. *Electronics, 11*(18), 2922.

[13] Habib, M., Khoucha, F., & Harrag, A. (2017). GA-based robust LQR controller for interleaved boost DC–DC converter improving fuel cell voltage regulation. *Electric Power Systems Research, 152*, 438-456.

[14] Riad, A. J., Hasanien, H. M., Ullah, Z., Alkuhayli, A., & Yakout, A. H. (2024). Voltage control of PEM fuel cell in a DC microgrid using optimal artificial rabbits algorithm-based fractional order PID controller. *IEEE Access, 12*, 89191-89204.

[15] Fathy, A., Ferahtia, S., Rezk, H., Yousri, D., Abdelkareem, M. A., & Olabi, A. G. (2022). Optimal adaptive fuzzy management strategy for fuel cell-based DC microgrid. *Energy, 247*, 123447.

[16] Xia, B., Guo, P., Wei, X., & Zong, H. (2023). Reaction gas pressure, temperature, and membrane water content modulate electrochemical process of a PEMFC: a simulation study. *Advances in Materials Science and Engineering, 2023*(1), 1346872.

[17] Manoharan, P., Ravichandran, S., Kavitha, S., Tengku Hashim, T. J., Alsoud, A. R., & Sin, T. C. (2024). Parameter characterization of PEM fuel cell mathematical models using an orthogonal learning-based GOOSE algorithm. *Scientific Reports, 14*(1), 20979.

[18] Ćalasan, M., Vujošević, S., Micev, M., Aleem, S. H. A., & Azzopardi, B. (2025). Advanced modeling and parameter estimation of PEM fuel cells using the g-function and self-adaptive differential evolution algorithm. *Scientific Reports, 15*(1), 44276.

[19] Divya, M., & Guruswamy, K. P. (2018). Design modelling and implementation of interleaved boost DC-DC converter. *International Journal of Innovative Science and Research Technology, 3*(2), 709–721.

[20] Kumar, R., Singh, R. K., Kumar, R., & Mishra, P. (2023). Design and simulation of interleaved boost converter. *International Journal for Research in Applied Science and Engineering Technology, 11*(1), 1760–1763.